



Published in final edited form as:

*Lab Chip*. 2012 November 7; 12(21): 4228–4231. doi:10.1039/c2lc40751e.

## Standing surface acoustic wave (SSAW) based multichannel cell sorting

Xiaoyun Ding<sup>a</sup>, Sz-Chin Steven Lin<sup>a</sup>, Michael Ian Lapsley<sup>a</sup>, Sixing Li<sup>a,b</sup>, Xiang Guo<sup>a</sup>, Chung Yu Keith Chan<sup>a</sup>, I-Kao Chiang<sup>a</sup>, Lin Wang<sup>c</sup>, J. Philip McCoy<sup>d</sup>, and Tony Jun Huang<sup>a,b</sup>

Tony Jun Huang: junhuang@psu.edu

<sup>a</sup>Department of Engineering Science and Mechanics, The Pennsylvania State University, University Park, PA 16802, USA. Fax: 814-865-9974; Tel: 814-863-4209

<sup>b</sup>Cell and Developmental Biology Program, The Pennsylvania State University, University Park, PA 16802, USA

<sup>c</sup>Ascent Bio-Nano Technologies Inc., State College, PA 16801, USA

<sup>d</sup>National Heart, Lung, and Blood Institute at NIH, Bethesda, MD 20892, USA

### Abstract

We introduce a novel microfluidic device for cell sorting in continuous flow using tunable standing surface acoustic waves. This method allows individual cells to be precisely directed into five different outlet channels in a single step. It is versatile, simple, label-free, non-invasive, and highly controllable.

Cell sorting is essential in numerous biological studies and clinical applications, such as molecular biology, pathology, immunology, genetics, and medical diagnostics and therapeutics.<sup>1,2</sup> Conventionally, cell sorting is performed by fluorescence-activated cell sorters (FACS), in which cells are encapsulated into small liquid droplets, which are then selectively labeled with electric charges and are sorted by an external electric field.<sup>3–6</sup> These droplet-based cell sorters, however, have several drawbacks: 1) they generate aerosols, thus requiring stringent protocols and precautions; 2) they require additional steps to enclose cells into droplets; 3) if one intends to post-process the cells after sorting (*e.g.*, cell culture), removing cells from droplets is necessary and often inconvenient. In this regard, it is important to develop other techniques that can perform direct cell-sorting without enclosing cells in droplets. In the past decade, researchers have developed several microfluidic-based methods for direct cell sorting, such as magnetic-activated cell sorting, optical tweezers, electrokinetic mobilization, and hydrodynamic flow.<sup>6–15</sup> These methods have pioneered many new avenues in on-chip cell sorting; however, they also suffer from drawbacks, such as limited controllability, low cell viability and proliferation, and/or requirements for bulky equipment.

Acoustic-based approaches appear to be excellent alternatives for cell sorting. Compared to their optical, electrical, or magnetic counterparts, acoustic-based manipulations<sup>16–35</sup> have been recognized as a more gentle approach to biological objects. Recently, acoustic-streaming-based droplet/cell sorting has been developed by utilizing the acoustically induced fluid streaming effect.<sup>36,37</sup> In this communication, we present a fundamentally different cell sorting method that is based on tunable standing surface acoustic waves

(SSAW). Our SSAW-based cell sorting method uses the acoustic radiation force to directly manipulate cells, rather than using the acoustic streaming effect to manipulate the fluids in which the cells are embedded. Because this method can precisely define and change the pressure nodes (PNs) of SSAW and thus the positions of cells (and designated outlets), and it does not involve acoustic streaming which is often chaotic and unpredictable, it can achieve more controllable and stable cell manipulation than the acoustic-streaming-based approaches. In addition, this method can produce a large range of translation ( $>100\ \mu\text{m}$ ). Our method's excellent controllability and large range of translation renders it capable of precisely sorting cells into a great number (*e.g.*, five) of outlet channels in a single step. This is a major advantage over most existing cell-sorting methods, which typically only sort cells into two outlet channels. In this work, we demonstrate the precise sorting of cells into five separate outlets in a single step without external labeling or droplet encapsulation. In addition, we conducted cell viability and proliferation tests to confirm the non-invasiveness of our approach.

Our SSAW-based cell-sorting device consists of a single-layer polydimethylsiloxane (PDMS) channel and a piezoelectric substrate with a pair of chirped IDTs, as shown in Fig. 1. We have previously demonstrated that particles/cells in a microfluidic channel can be statically patterned in a SSAW field.<sup>18</sup> They were driven by the acoustic radiation force to the PNs or anti-nodes (ANs) of the SSAW, depending on their material properties. To acoustically sort particles/cells, however, one must be able to dynamically move the position of PNs/ANs. In this work, we achieve the manipulation of PNs/ANs through generation of a tunable SSAW using chirped IDTs. The gradient in IDT pitch allows the excitation of SAWs over a wide range of frequencies.<sup>22,38,39</sup> Therefore, by tuning the frequency of SSAW, we can precisely move the PNs/ANs in the lateral direction normal to the cell flow, which in turn drives the floating cells to designated outlets on the fly (Figs. 1a & 1b).

Figure 2a shows a photographic image of our device. We used  $128^\circ$  Y-cut  $\text{LiNbO}_3$  as the substrate for its optical transparency and excellent electrical-mechanical coupling efficiency. The electrodes of the chirped IDT are aligned parallel to the X-axis of the  $\text{LiNbO}_3$  substrate. The pitch of the chirped IDT electrodes ranges linearly from  $140\ \mu\text{m}$  to  $200\ \mu\text{m}$ , producing a working frequency range of  $\sim 9.5\ \text{MHz}$  to  $\sim 14.5\ \text{MHz}$ . The distance between the two chirped IDTs is  $17\ \text{mm}$ . The sorting device was mounted on the stage of an inverted microscope (Nikon TE2000U). A radio frequency (RF) signal was generated by a function generator (Agilent E4422B) to drive the two chirped IDTs simultaneously. Solutions of human white blood cells (HL-60,  $\sim 10\ \mu\text{m}$  in diameter), or fluorescent polystyrene beads (dragon green) with diameters of  $15$  and  $10\ \mu\text{m}$ , were injected into the microfluidic channel by syringe pumps (NEMESYS) and hydrodynamically focused to the center of the main channel by two side sheath flows before the RF signals were applied to the IDTs. The flow rates of sample flow and the sheath flow were  $0.2\ \mu\text{l}/\text{min}$  and  $1.0\ \mu\text{l}/\text{min}$ , respectively. The solution we used was phosphate buffered saline (PBS). A CCD camera (CoolSNAP HQ2, Photometrics, Tucson, AZ) was connected to the microscope to monitor the sorting process.

The SSAW field is formed by the two parallel chirped IDTs on the surface of the substrate (underneath the microfluidic channel). The SSAW couples into the liquid medium and generates an acoustic radiation force on objects suspended in the liquid. The density and compressibility of the object and the surrounding liquid determine whether the objects will be driven to the PNs or ANs; however, most objects suspended in aqueous solutions, including polystyrene beads and blood cells, will be pushed to the PNs.<sup>16–22</sup> The PN location is determined by the SAW wavelength, which is directly dependant on the signal frequency  $f$  ( $f = c/\lambda$ , where  $c$  is the SAW velocity on the surface of the substrate). Note that the PN at the center of the two chirped IDTs is fixed (independent of frequency) and is therefore referred as 0 order. The subsequent PNs progressing outward from the 0 order are

deemed the 1<sup>st</sup> order, 2<sup>nd</sup> order, 3<sup>rd</sup> order, *etc.* All other ( $n > 0$ ) PNs can be moved simply by modulating the applied signal frequency; however, the node movement varies at different

orders. The node movement ( $\Delta x_n$ ) can be described by: 
$$\Delta x_n = \frac{n(\lambda_i - \lambda_j)}{2} = \frac{n\left(\frac{c}{f_i} - \frac{c}{f_j}\right)}{2},$$
 where  $i, j > 0$ . As shown in Fig. 1, we arranged PNs and ANs parallel to the channel walls. The center of the microchannel is located at a distance of around 1500  $\mu\text{m}$  ( $5\lambda$  at 14 MHz) from the 0 order mode. Simply by varying the input frequency applied to the chirped IDTs, we can shift the location of the PNs. As a result, particles/cells trapped in the PN can be translated laterally across the channel, and with the addition of a fluid flow, the particles/cells can be directed into any of the upper or lower output channels, which correspond to certain input frequency, as shown in Fig. 1(a & b).

Our sorting device was first characterized by its sorting distance. Figure 1c is the merged trajectories of 10  $\mu\text{m}$  polystyrene particles moving through the sorting region at frequencies of 9.8 MHz and 10.1 MHz. A lateral shift of  $\sim 100 \mu\text{m}$  was achieved at the end of the sorting region. Note that due to the wide working frequency range of the chirped IDT, precise alignment of PDMS channel and IDTs are not required. With further optimization on the chirped IDT, a lateral shift greater than 100  $\mu\text{m}$  can be obtained for applications that require larger sorting distances.

To demonstrate the functionality of our SSAW-based sorting method, we first sorted 15  $\mu\text{m}$  fluorescent polystyrene beads (dragon green, Bangs Lab) with a density of 1.05  $\text{g}/\text{cm}^3$  to 3 outlet channels. In this experiment, the width and height of the main channel were 200  $\mu\text{m}$  and 70  $\mu\text{m}$ , respectively. When SSAW was off, the particles did not experience any acoustic force and thus followed the flow to the center outlet channel (center image of Fig. 2b). When an input signal was applied with a frequency of 14.5 MHz, the closest PN to the particles was  $\sim 25 \mu\text{m}$  above the center of the channel and directed particles to the upper outlet channel (top image of Fig. 2b). When the frequency was switched to 13.9 MHz, the PN was positioned below the center of the channel and particles were directed to the lower outlet channel (bottom image of Fig. 2b). These images were produced by stacking a video which captured the continuous particle-sorting process. The particle velocity in the main channel in our experiment was  $\sim 2000 \mu\text{m}/\text{s}$ , and the power applied to the device was  $\sim 25 \text{ dBm}$ .

To further demonstrate the versatility of our method and its ability to sort cells into more outlets, we tested human white blood cells (HL-60 human promyelocytic leukemia cells) in our sorting device. The leukemia cells were first hydrodynamically focused to the center of the main channel by two side flows, and then sorted to five specific outlets at frequencies of 9.8, 10.0, 10.2, 10.6, and 10.9 MHz, respectively. The cell-sorting results are shown in Fig. 3 by stacking the images of experimental videos recorded under the various frequencies described above. Our device was able to sort cells into five individual outlets on a single microfluidic chip. We could potentially extend from the current five outlets to a higher number of outlet channels to increase the functionality of the device for applications such as whole blood analysis and antigen-based cell diagnostics, where the separation of many cell types is necessary. We have also conducted standard cell viability and proliferation assays to prove the non-invasive nature of our SSAW-based technique.<sup>22</sup> HeLa cells showed no significant sign of decrease in both viability and proliferation after exposure to SSAW fields for 10 min, implying no significant physiological damage was induced by our technique.

In conclusion, we have demonstrated a tunable SSAW-based cell sorting technique that can sort cells into five outlets in a continuous flow, rendering it particularly desirable for multi-type cell sorting. Our device is assembled on a low-cost and disposable microfluidic chip and requires small sample volumes ( $\sim 100 \mu\text{l}$ ), making it an ideal tool for research labs and

point-of-care diagnostics. Furthermore, it can be conveniently integrated with a small RF power supply, a fluorescent detection module, and a high-speed electrical feedback module to function as a fully integrated, portable, inexpensive, multi-color, miniature fluorescence-activated cell sorting ( $\mu$ FACS) system.

## Acknowledgments

This research was supported by National Institutes of Health (NIH) Director's New Innovator Award (1DP2OD007209-01), National Science Foundation (NSF), NSF Graduate Research Fellowship (Grant No. DGE-0750756), and the Penn State Center for Nanoscale Science (MRSEC). Components of this work were conducted at the Penn State node of the NSF-funded National Nanotechnology Infrastructure Network. We thank Dr. Bernhard R. Tittmann and Brian Reinhardt for their assistance with equipment.

## Notes and references

- Eisenstein M. *Nature*. 2006; 441:1179–1185. [PubMed: 16810261]
- Shapiro, HM. *Practical flow cytometry*. Wiley-Liss; New York: 2003.
- Leary JF. *Cytometry*. 2005; 67A:76–85. [PubMed: 16163688]
- Baret JC, Miller OJ, Taly V, Ryckelynck M, El-Harrak A, Frenz L, Rick C, Samuels ML, Hutchison JB, Agresti JJ, Link DR, Weitz DA, Griffiths AD. *Lab Chip*. 2009; 9:1850–1858. [PubMed: 19532959]
- Gomez, FA. *Biological Applications of Microfluidics*. 1. John Wiley & Sons; Hoboken, NJ: 2008.
- Salieb-Beugelaar GB, Simone G, Arora A, Philippi A, Manz A. *Anal Chem*. 2010; 82:4848–64. [PubMed: 20462184]
- Chen CH, Cho SH, Chiang H-I, Tsai F, Zhang K, Lo YH. *Anal Chem*. 2011; 83:7269–7275. [PubMed: 21809842]
- Wang X, Chen S, Kong M, Wang Z, Costa KD, Li Ra, Sun D. *Lab Chip*. 2011; 11:3656–62. [PubMed: 21918752]
- Plouffe BD, Mahalanabis M, Lewis LH, Klapperich CM, Murthy SK. *Anal Chem*. 2012; 84:1336–44. [PubMed: 22240089]
- Forbes TP, Forry SP. *Lab Chip*. 2012; 12:1471–1479. [PubMed: 22395226]
- Shen F, Hwang H, Hahn YK, Park JK. *Anal Chem*. 2012; 84:3075–81. [PubMed: 22380761]
- Beech JP, Holm SH, Adolfsson K, Tegenfeldt JO. *Lab Chip*. 2012; 12:1048–51. [PubMed: 22327631]
- Wu TH, Chen Y, Park SY, Hong J, Teslaa T, Zhong JF, Carlo DD, Teitell MA, Chiou PY. *Lab Chip*. 2012; 12:1378–83. [PubMed: 22361780]
- Beech JP, Holm SH, Adolfsson K, Tegenfeldt JO. *Lab Chip*. 2012; 12:1048–51. [PubMed: 22327631]
- Carlo DD, Irimia D, Tompkins RG, Toner M. *Proc Natl Acad Sci USA*. 2007; 104:18892. [PubMed: 18025477]
- Dual J, Hahn P, Leibacher I, Möller D, Schwarz T. *Lab Chip*. 2012; 12:852–62. [PubMed: 22301707]
- Bruus H. *Lab Chip*. 2012; 12:1014–21. [PubMed: 22349937]
- Shi J, Ahmed D, Mao X, Lin SCS, Lawit A, Huang TJ. *Lab Chip*. 2009; 9:2890–5. [PubMed: 19789740]
- Glynn-Jones P, Boltryk RJ, Hill M. *Lab Chip*. 2012; 12:1417–1426. [PubMed: 22402608]
- Wiklund M. *Lab Chip*. 2012; 12:2018–2028. [PubMed: 22562376]
- Shi J, Yazdi S, Lin SCS, Ding X, Chiang IK, Sharp K, Huang TJ. *Lab Chip*. 2011; 11:2319–24. [PubMed: 21709881]
- Ding X, Lin SS, Kiraly B, Yue H, Li S, Chiang IK, Shi J, Benkovic SJ, Huang TJ. *Proc Natl Acad Sci USA*. 2012; 109:11105–09. [PubMed: 22733731]
- Johansson L, Nikolajeff F, Johansson S, Thorslund S. *Anal Chem*. 2009; 81:5188–96. [PubMed: 19492800]

24. Patel MV, Tovar AR, Lee AP. *Lab Chip*. 2012; 12:139–45. [PubMed: 22072298]
25. Vanherberghen B, Manneberg O, Christakou A, Frisk T, Ohlin M, Hertz HM, Önfelt B, Wiklund M. *Lab Chip*. 2010; 10:2727–32. [PubMed: 20820481]
26. Lee C, Lee J, Kim HH, Teh S-Y, Lee A, Chung I-Y, Park JY, Shung KK. *Lab Chip*. 2012; 12:1039/C2LC21123H
27. Shi J, Mao X, Ahmed D, Colletti A, Huang TJ. *Lab Chip*. 2008; 8:221–3. [PubMed: 18231658]
28. Lenshof A, Laurell T. *Chem Soc Rev*. 2010; 39:1203–1217. [PubMed: 20179832]
29. Wang Z, Zhe J. *Lab Chip*. 2011; 11:1280–1285. [PubMed: 21301739]
30. Shi J, Huang H, Stratton Z, Huang Y, Huang TJ. *Lab Chip*. 2009; 9:3354–9. [PubMed: 19904400]
31. Ding X, Shi J, Lin SCS, Yazdi S, Kiraly B, Huang TJ. *Lab Chip*. 2012; 12:2491–2497. [PubMed: 22648600]
32. Reboud J, Wilson R, Zhang Y, Ismail MH, Bourquin Y, Cooper JM. *Lab Chip*. 2012; 12:1268–73. [PubMed: 22327572]
33. Rezk AR, Qi A, Friend JR, Li WH, Yeo LY. *Lab Chip*. 2012; 12:773–779. [PubMed: 22193520]
34. Petersson F, Aberg L, Swärd-Nilsson AM, Laurell T. *Anal Chem*. 2007; 79:5117–23. [PubMed: 17569501]
35. Liu YJ, Ding X, Lin SS, Shi J, Chiang I, Huang TJ. *Advanced Materials*. 2011; 23:1656–1659. [PubMed: 21438028]
36. Franke T, Braunmüller S, Schmid L, Wixforth a, Weitz DA. *Lab Chip*. 2010; 10:789–794. [PubMed: 20221569]
37. Franke T, Abate AR, Weitz DA, Wixforth A. *Lab Chip*. 2009; 9:2625–2627. [PubMed: 19704975]
38. Lin SCS, Mao X, Huang TJ. *Lab Chip*. 2012; 12:2766–2770. [PubMed: 22781941]
39. Campbell, CK. *Surface Acoustic Wave Devices for Mobile and Wireless Communications*. 1. Academic; San Diego: 1998.

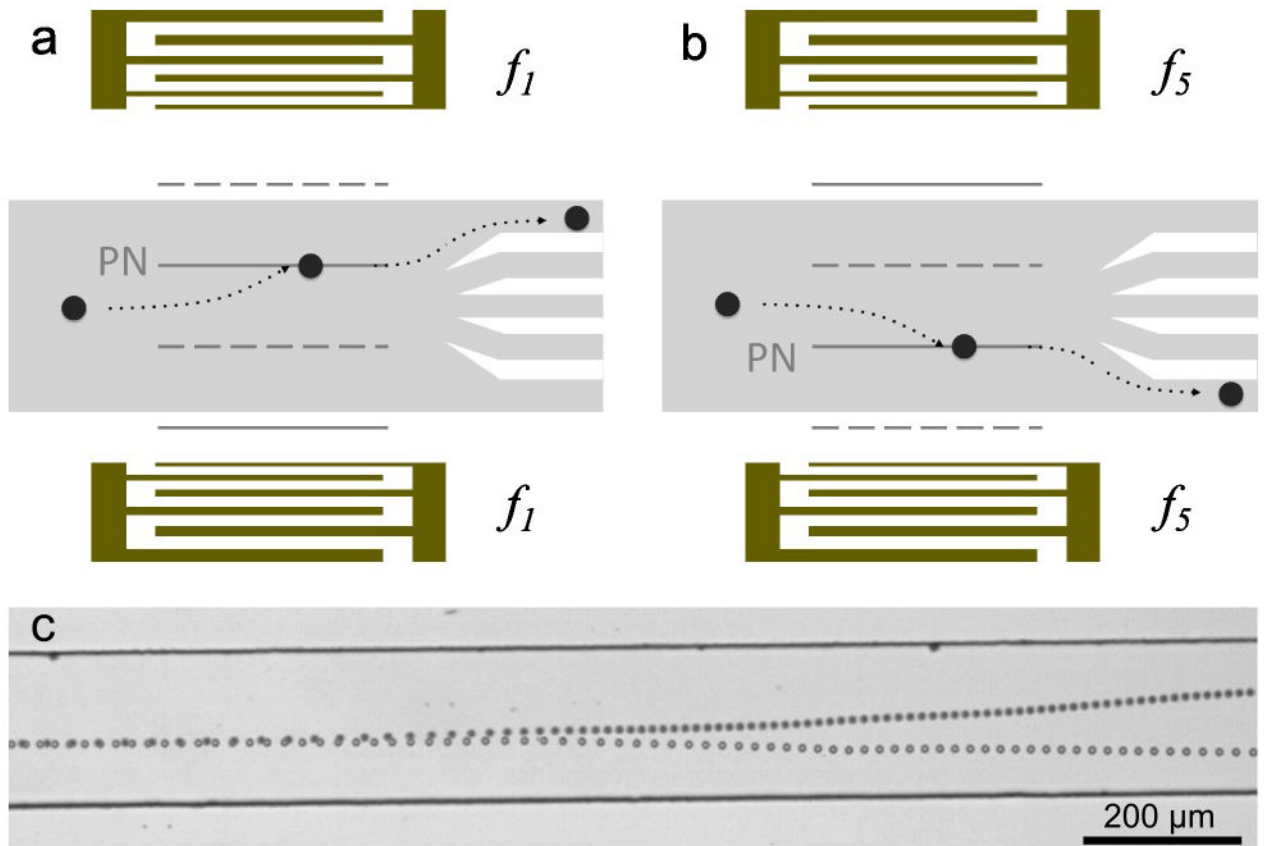


**Figure 1.**

(a,b) Working mechanism of the SSAW-based cell-sorting device. When the SSAW is switched on at frequency of (a)  $f_1$  and (b)  $f_5$ , all particles/cells are driven to the pressure node (solid lines) and directed in the (a) upper or (b) bottom outlet. (c) The stacked trajectories of two  $10\ \mu\text{m}$  polystyrene beads at two frequencies respectively in the SSAW working region. A lateral shift of  $100\ \mu\text{m}$  is achieved after passing through the cell-sorting region.

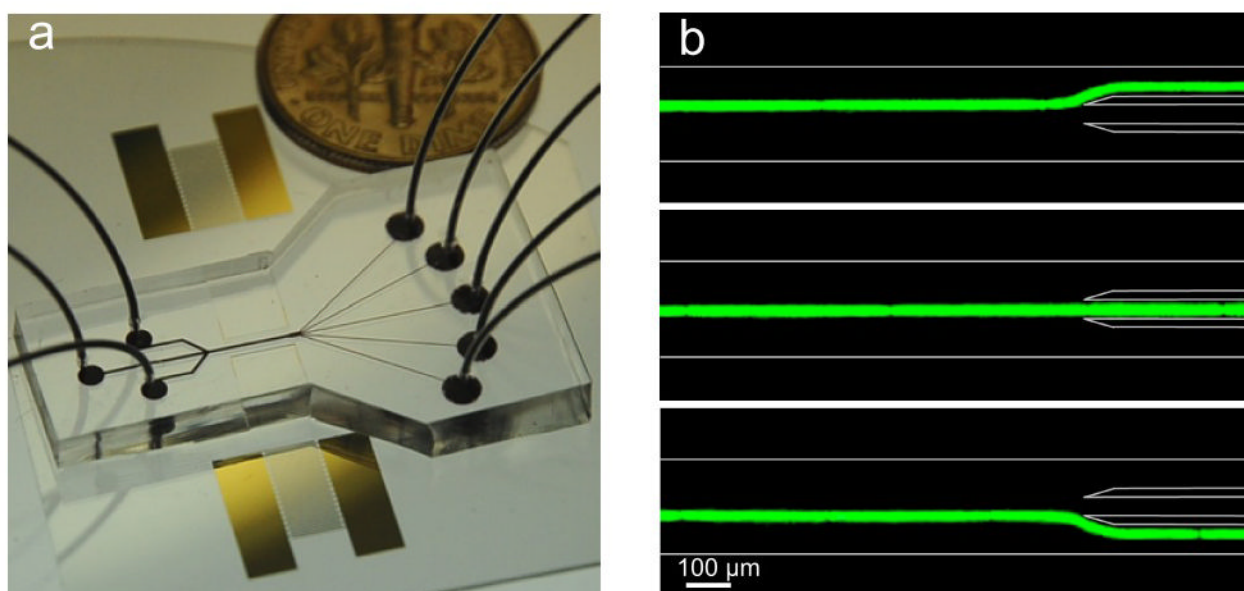


**Figure 2.** (a) An optical picture of the SSAW-based cell-sorting device with 3 inlets and 5 outlets. (b) A 15  $\mu\text{m}$  fluorescent particle passing through the sorting region can be directed to three different outlet channels by modulating input frequency (14.5 MHz, SAW off, and 13.9 MHz).

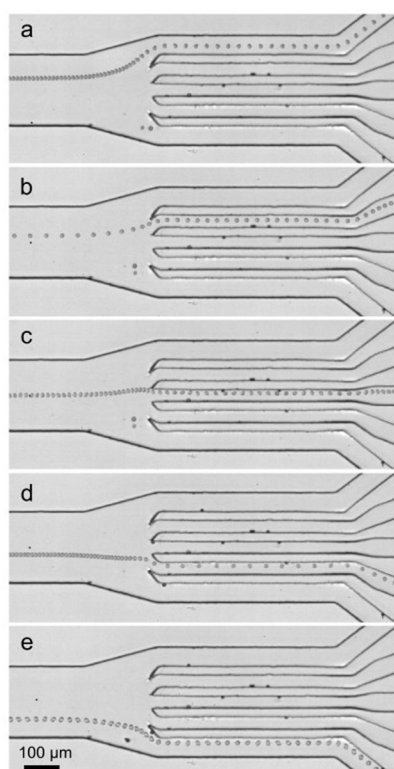


**Figure 3.** Sorting of human white blood cells (HL-60 human promyelocytic leukemia cells) into five specific outlet channels at frequencies of (a) 9.8, (b) 10.0, (c) 10.2, (d) 10.6, and (e) 10.9 MHz.